DOI: 10.17725/rensit.2022.14.065

Noise signal detection by horizontal antenna in ocean waveguide

Venedikt M. Kuz'kin
Prokhorov General Physics Institute of RAS, http://www.gpi.ru/
Moscow 119991, Russian Federation
E-mail: kumiov@yandex.ru

Sergey A. Pereselkov, Sergey A. Tkachenko, Dmitry Yu. Prosovetskii
Voronezh State University, http://www.vsu.ru/
Voronezh 394006, Russian Federation
E-mail: pereselkov@yandex.ru, tkachenko.edu@yandex.ru, dmitry.prosovetskii@yandex.ru

Yury V. Matvienko
Institute of Marine Technology Problems, Far Eastern Branch of RAS, http://www.febras.ru/
Vladivostok 690091, Russian Federation
E-mail: ymat@marine.febras.ru

Received 14 March, 2022, peer-reviewed 21 March, 2022, accepted 25 March, 2022

Abstract: **Interferometric processing of hydroacoustic information by using a horizontal linear antenna is described. The detection of a noise source signal is considered by using the Neumann-Pearson criterion. The expressions for the probability of correct detection and false alarm are obtained as dependence on the signal/noise ratio and the number of antenna elements. Numerical calculations are performed. The curves of the probability of noise signal detection are given. The efficiency of signal detection by using an antenna in relation to a single receiver is estimated.**

Keywords: **dispersion, interferometry, noise source, Neumann-Pearson criterion, detection parameters, horizontal antenna, modeling**

UDC 004.052.34

Acknowledgments: This work was supported by grants from the Russian Foundation for Basic Research (project 19-29-06075). The work of D.Yu. Prosovetskii was supported by the grant of the President of the Russian Federation MK-6144.2021.4.

For citation: Venedikt M. Kuz'kin, Sergey A. Pereselkov, Yury V. Matvienko, Sergey A. Tkachenko, Dmirty Yu. Prosovetskii. Noise signal detection by horizontal antenna in oceanic waveguide. *RENSIT: Radioelectronics. Nanosystems. Information Technologies,* 2022, 14(1)65-72. DOI: 10.17725/rensit.2022.14.065.

Contents

1. **Introduction (65)**
2. **Interferometric processing (66)**
3. **Processing immunity (68)**
4. **Detection of a noise signal according to the neumann-pearson criterion (68)**
   - **4.1. Detection curves for single receiver (68)**
   - **4.2. Detection curves for antenna (68)**
5. **Numerical simulation (69)**
6. **Conclusion (70)**

References (71)

1. INTRODUCTION

Waveguide dispersion and multimode propagation in ocean waveguides determines special method of broadband sound source localization in ocean waveguide. It based on stable structural features formed by the interferogram [1,2]. The interferogram is squared absolute value of signal amplitude in frequency-distance (time) domain. First steps in solving source localization problem were presented in papers [3-8], where particular

solutions of inverse problem are suggested with using such parameter as waveguide invariant coined in [1]. However, they are ineffective in conditions of small ratio signal/noise (s/n).

Interferometric processing for solving complex broadband source location problem (detection, direction finding, radial velocity determination (velocity projection toward the receiver), moving away, depth and resolution of several sources), stable for parameters variations of ocean environment, is suggested and proved in papers [9-14]. Processing realizes multiple quasicoherent accumulating of wave field spectral density along located interferometric fringes in frequency-time domain. During the period of observation Δt in source band Δω J independent realizations t_s duration with time range δt_s between them are accumulated

$$J = \frac{\Delta t}{t_s + \delta t_s}. \quad (1)$$

Realizations are independent, if $\delta t_s > 2\pi/\Delta\omega$. The interferogram forms in frequency-time domain and then two-dimensional Fourier transform (2D-FT) is applied in time-frequency domain. Transformed integrated density spectrum we call hologram. It consists of few focal spots in small area. Spots are the result of the interference of modes with different wavenumbers. Contrary to noise signal noise addition is incoherent and noise distribution fills all hologram area. It bring about high-noise-immunity processing. Determine of radial velocity and source removing away from receiver is based on information about maxima of focal spots coordinates [10,11,14]. Problems about depth, bearing, source resolution determination are considered in [9,12,13]. For single receiver noise signal detection based on Neiman-Pearson test using interferometric processing described in [15].

Presently much attention is given to using of small submersibles in maritime security operations [16]. The effective detection of weak signals by these submersibles involves the use of small antennas.

The purpose of this work is building a theory of noise signal detection using a receiving horizontal linear antenna. Numerical simulation results for small antennas are presented.

2. INTERFEROMETRIC PROCESSING

Interferometric processing with using of horizontal linear antenna is considered in [17]. The layout of source S and horizontal linear antenna is shown in the **Fig. 1**. Number of space-regular antenna elements Q_b is B, $b = \overline{1, B}$, interelement spacing – d. Antenna elements are located at a depth z_q. The first element Q_1 is chosen as a reference. The aperture $L = (B - 1)d$ is much less then distance to the source, $L << r_b$. In this case $r_b = r_1 - (b - 1)d\sin\theta$, where θ – angle complementary to bearing. The source at fixed depth z_s moves with constant velocity v. The signal spectrum ranges in band $-(\Delta\omega/2) + \omega_0 \le \omega \le \omega_0 + (\Delta\omega/2)$, $\omega = 2\pi f$ circular frequency.

Fields from antenna elements are summed up. In the process distance difference from the source to different antenna elements in direction of angle θ is compensated. That's why field of b-th element multiplied by $\exp[ih_*(\omega_0)(b - 1)d\sin\theta_*]$. Here $h_*(\omega_0)$ – singled-out real part of horizontal wavenumber (propagation constant) on average source spectrum frequency ω_0, θ_* – compensation angle. Outlet field from b-th antenna element can be presented in the form of sum by discrete spectrum modes as [18]

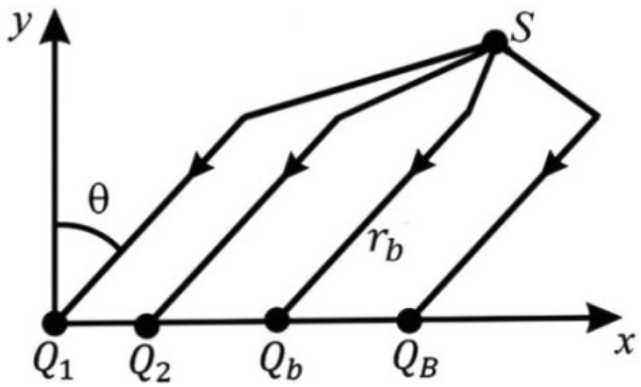

Fig. 1. *Geometry of the problem (top view): r_b – horizontal distance of the element Q_b to the source S, θ – angle of direction to the source.*

$$p_b(\omega, r_1, z_{s,q}, \theta, \theta_*) = \sum_m A_m(\omega, r_1, z_{s,q}, \theta, \theta_*) \times$$
$$\times \exp\{i[h_m(\omega) r_1 - 2(b-1)(h_m(\omega)\eta - h_*(\omega_0)\eta_*)]\}, \quad (2)$$
$$\eta = d \sin\theta / 2, \quad \eta_* = d \sin\theta_* / 2,$$

A_m and h_m – the amplitude and the constant of m-mode propagation. Cylindrical field divergence, modal attenuation, source and antenna elements depths z_s and z_b respectively, are taken into account formal by modes amplitude dependence. Then source and receivers depths arguments at the received signal are omitted. In antenna output the field is

$$p_{an}(\omega, r_1, \theta, \theta_*) = \sum_b p_b(\omega, r_b, \theta, \theta_*). \quad (3)$$

In the interferogram $P_{an}(\omega, r_1, \theta, \theta_*) = |p_{an}(\omega, r_1, \theta, \theta_*)|^2$ we turn from distance variable to time variable and apply two-dimensional Fourier transform

$$F_{an}(\tilde{\nu}, \tau, \theta, \theta_*) =$$
$$= \int_0^{\Delta t} \int_{\omega_0 - \frac{\Delta\omega}{2}}^{\omega_0 + \frac{\Delta\omega}{2}} P_{an}(\omega, t, \theta, \theta_*) \exp[i(\tilde{\nu} t - \omega\tau)] dt d\omega, \quad (4)$$

where $\tilde{\nu} = 2\pi\nu$ и τ – circular frequency and hologram time, Δt – observing time. At moment $t_0 = 0$ starting distance is $r_1 = r_0$.

The efficiency of interferometric processing using antenna with respect to the single receiver we characterize by amplification gain factor

$$\chi = |G_{an}(B, \theta, \theta_*)| / |G_r|, \quad (5)$$

and и directional characteristic

$$D(B, \theta, \theta_*) = G_{an}(B, \theta, \theta_*) / \max G_{an}. \quad (6)$$

Here

$$G_{an}(B, \theta, \theta_*) = \iint_U |F_{an}(\tau, \tilde{\nu}, \theta, \theta_*)| d\tau d\tilde{\nu}, \quad (7)$$

$$G_r = \iint_U |F_r(\tau, \tilde{\nu})| d\tau d\tilde{\nu}. \quad (8)$$

Index «*r*» here and below relates to single receiver, U – hologram spectral density localization area (dotted line in **Fig. 2***b,d*).

Increase in the number B of antenna elements peaks primary maxima of antenna directional characteristic, remain constant their position,

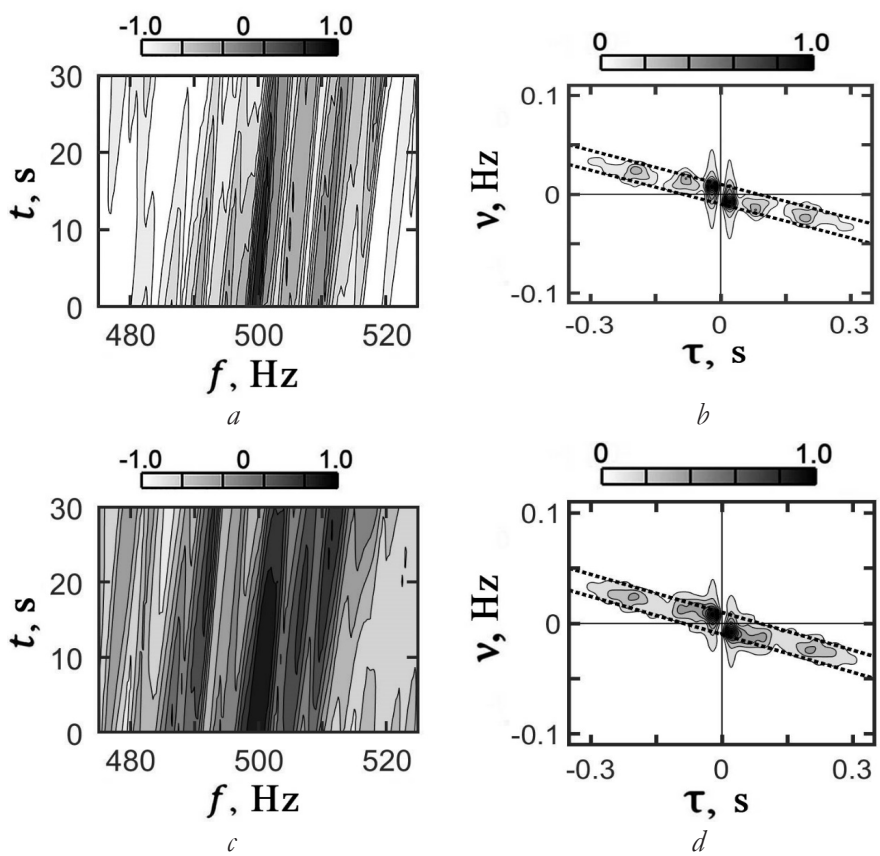

Fig. 2. *Normalized interferograms (a, c) and holograms (b, d) of a single receiver (a, b) and a seven-element antenna (c, d) in the absence of noise.*

and leads to secondary maxima increment. With compensation angle θ_* rising width of primary maxima of directional characteristic increases. The greatest width is at value $\theta_* = 90°$. Maximum value of amplification gain factor, approximately equal B^2, achieved in direction of the compensation angle.

3. PROCESSING IMMUNITY

It is convenient to characterize processing immunity by limiting input ratio s/n q_{lim}, when stable detection is provided and parameter estimates are close to real values. In the case of single receiver and isotropic noise for scalar field component we have $q_{\text{lim}}^{(r)} \approx 1.5 / J^2$.

Assume that noise signal and noise are stochastic processes, not statistically related, and noise at input of antenna elements is not correlated. The second condition is met, if $d \geq \lambda/2$, where λ – wavelength. Then limiting input ratio s/n on antenna element is evaluated as

$$q_{\text{lim}}^{(an)} = \alpha q_{\text{lim}}^{(r)}, \quad (9)$$

where $\alpha = B/\chi$. The greatest value is $\chi_{\max} \approx B^2$, so $\alpha_{\min} \approx 1/B$. Considering the above $\min q_{\text{lim}}^{(an)} \approx q_{\text{lim}}^{(r)} / B$. Input ratio s/n on singular antenna is limited by inequality $q_0 \geq q_{\text{lim}}^{(an)}$.

4. DETECTION OF A NOISE SIGNAL ACCORDING TO THE NEUMANN-PEARSON CRITERION

Neumann-Pearson criterion maximizes the probability of correct detection of p_1 for a given probability of false alarm p_2. When considering the problem of detecting a noise signal (pressure), we will limit ourselves to the area of the input relations s/n $q_0 \geq q_{\text{lim}}$.

4.1. Detection curves for single receiver [15]

The probability of a false alarm $p_2^{(r)}$, as the probability of exceeding the pore level g_r by noise, is equal to

$$p_2^{(r)} = 1 - 0.5\left[\Phi(k_n^{(r)} - 0.5) + \Phi(k_n^{(r)} + 0.5)\right], \quad (10)$$

where is the dimensionless parameter $k_n^{(r)} = g_r / 2M_n^{(r)}$, $M_n^{(r)}$ – mathematical expectation of noise at the processing output, $\Phi(x)$ – error integral

$$\Phi(x) = \frac{2}{\sqrt{\pi}} \int_0^x e^{-t^2} dt. \quad (11)$$

Given the probability of a false alarm $p_2^{(r)}$ the parameter $k_n^{(r)}$ is uniquely determined. With $k_n^{(r)}$ decreasing in the probability of a false alarm, according to (10), (11), the value of $k_n^{(r)}$ increases. The maximum value of the parameter $k_n^{(r)}$ is estimated as $\max k_n^{(r)} \approx 4$.

Probability of correct detection $p_1^{(r)}$

$$p_1^{(r)} = 1 - 0.5\left[\Phi(\eta_1^{(r)}) + \Phi(\eta_2^{(r)})\right], \quad (12)$$

where

$$\eta_1^{(r)} = \frac{2k_n^{(r)} - 1 - q_r}{2(1+q_r)}, \ \eta_2^{(r)} = \frac{2k_n^{(r)} + 1 + q_r}{2(1+q_r)}, \quad (13)$$

$q_r = J\gamma_r q_0$ – s/n ratio at the processing output. Here $\gamma_r = S_n^{(r)} / S_s^{(r)}$ – compression ratio, $S_{s,n}^{(r)}$ – is the area of distribution of the spectral density of the signal and noise on the hologram. Probability of correct detection $p_1^{(r)}$ is uniquely determined by the parameter $k_n^{(r)}$ and the s/n ratio q_r. Thus, it is possible to calculate the detection curves of the noise signal. They represent the dependence of the probability of correct detection on the output (or input) s/n ratio with a fixed probability of a false alarm.

4.2. Detection curves for antenna

Expressions for the probabilities of false alarm $p_2^{(r)}$ (10) and correct detection $p_1^{(r)}$ (12) are also preserved for the antenna with the only difference that the values of the arguments that characterize them change. With a fixed probability of false alarm, $p_2^{(an)} = p_2^{(r)} = p_2$, the dimensionless parameter k_n is constant, $k_n^{(r)} = k_n^{(an)} = k_n$. Compared with a single receiver, the mathematical expectation of noise at the processing output increases by B times, $M_n^{(an)} = BM_n^{(r)}$. This leads to an increase in the pore level also by B times, $g_{an} = Bg_r$. Taking into account these observations, the probability of correct detection is equal to

$$p_1^{(an)} = 1 - 0.5\left[\Phi(\eta_1^{(an)}) + \Phi(\eta_2^{(an)})\right], \quad (14)$$

rAe

$$\eta_1^{(an)} = \frac{2k_n - 1 - q_{an}}{2(1+q_{an})},\ \eta_2^{(an)} = \frac{2k_n + 1 + q_{an}}{2(1+q_{an})}. \qquad (15)$$

Here $q_{an} = (J\gamma_{an}(B)/\alpha)q_0$ – is the s/n ratio at the processing output, where $\gamma_{an}(B)$ – compression ratio. It is determined similarly to a single receiver and does not depend on the viewing angle θ, the values $\gamma_{an} = \gamma_r = \gamma$ [17]. Compared with a single receiver, the output ratio of s/n increases by about B times.

The degree of difference in the probabilities of correct detection between a single receiver and an antenna, depending on the input s/n ratio and the number of antenna elements for a given false alarm probability, will be characterized by the ratio

$$\beta(q_0, B) = p_q^{(an)}(q_0, B) / p_1^{(r)}(q_0). \qquad (16)$$

The parameter $\beta(q_0,B)$ (16) is called the efficiency coefficient. When considering the efficiency coefficient $\beta(q_0,B)$, the area of input relations s/n q_0 is limited to the area of values $q_0 \geq q_{\lim}^{(r)}$.

5. NUMERICAL SIMULATION

A horizontally homogeneous waveguide with a depth of $H = 70$ *m*, a sound velocity constant in depth $c = 1480$ *m/s*. Frequency range $\Delta f = 480$–520 Hz. The average frequency of the spectrum $f_0 = 500$ Hz. Parameters of the absorbing liquid homogeneous bottom: the ratio of the density of soil and water $\varrho = 1.8$, the complex refractive index $n = 0.84(1 + i0.04)$.

The number of antenna elements B = 3, 7, 11. The interelement distance $d = 1.5$ *m*. It approximately corresponds to half the wavelength at a frequency of $f_0 = 500$ Hz. The elements of the horizontal antenna are located at a depth of $z_b = 50$ *m*. Angles: $\theta = 0°$, 30°, 60°, 90°. The allocated propagation constant is equal to the propagation constant of the first $h_*(f_0) = h_1(f_0) = 2.1182\ m^{-1}$. According to numerical calculations, the antenna gain coefficients χ do not depend on the viewing angle θ and are equal to: 8.7 ($B = 3$), 47.9 ($B = 7$), 119.3 ($B = 11$). They are close to the theoretical estimate $\chi = B^2$.

The noise source is located at a depth of $z_s = 20$ *m* and was moving away from the antenna with a radial velocity $w = 2$ *m/s*. At the initial time $t_0 = 0$, the source is removed from the antenna reference element Q_1 by a distance $r_0 = 10$ km. Accumulation time Δt = 30 *s*, duration of noise realization $t_s = 2$ *s*, time interval $\delta t_s = 0.5$ *s*, number of realizations J = 12. Limiting input c/n ratios: when using a single receiver $q_{\lim}^{(r)} \approx 10^{-2}(-20dB)$. When using the antenna: a) $B = 3$, $q_{\lim}^{(an)} \approx 3.4 \cdot 10^{-3}(-24,7dB)$; *b*) $B = 7$, $q_{\lim}^{(an)} \approx 1.5 \cdot 10^{-3}$(-28.2 dB); c) $B = 11$, $q_{\lim}^{(an)} \approx 9.2 \cdot 10^{-4}$(-30.4 dB). False alarm probabilities $p_2 = 10^{-1}, 10^{-2}, 10^{-3}$.

The illustrative material is shown in **Fig. 2-5**. **Fig. 2** demonstrates normalized interferograms and hologram modules in the absence of noise for a single receiver of a seven-element antenna. In order to increase the contrast on the interferograms, the constant components (background) for the modes of numbers $m = n$ are filtered out. If the constant components are not subtracted from the interferograms before applying the Fourier transform, then a peak of high intensity will appear on the holograms in the area of the origin. The spectral density localization area on holograms (Fig. 2*b,d*) is highlighted with a dotted line. From Fig. 2*b,d* it follows that the geometry of the location of the spectral density of a single receiver and antenna, regardless of the viewing angle, are close to each other. This result does not depend on the number of antenna elements. According to Fig. 2*b,d*, the compression ratio is estimated as $\gamma = 6$.

Fig. 3 shows the noise signal detection curves for a single receiver. As the probability of a false alarm decreases, the probability of correct detection decreases. According to the calculation results, the parameter $k_n = 1.42$ ($p_2 = 0.1$), $k_n = 2.14$ ($p_2 = 0.01$), $k_n = 2.72$ ($p_2 = 0.001$).

The curves for detecting a noise signal using an antenna are shown in **Fig. 4**. According to numerical simulation data, they do not depend on the viewing angle θ. Fig. 4*a,b,c* show how the

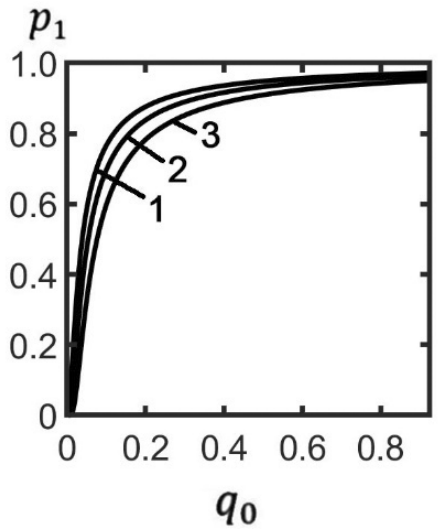

Fig. 3. *Dependence of the probability of correct detection p_1 on the input ratio s/n q_0 for various values of false alarm probabilities p_2: curve 1 – p_2 = 0.1, curve 2 – p_2 = 0.01, curve 3 – p_2 = 0.001. Single receiver.*

probabilities of correct detection of p_1 increase with an increase in the number of antenna elements *B*. For example, for the probability of a false alarm p_2 = 0.001, the probability of correct detection p_1 = 0.8 is achieved for the input s/n ratio q_0 = 0.044 at *B* = 3, q_0 = 0.019 at *B* = 7, q_0 = 0.012 at *B* = 11.

Fig. 5 shows the dependences of the efficiency coefficient $\beta(q_0)$ for different values of false alarm probabilities p_2 and the number of antenna elements *B*. The difference in the probabilities of correct detection between a single receiver and an antenna is concentrated mainly in the area of small s/n ratios q_0 and with an increase in the number of elements *B*, the difference increases. With increasing values of q_0, this difference decreases and asymptotically tends to zero.

6. CONCLUSION

The problem of detecting a weak signal in the presence of intense noise is topical in hydroacoustics. The difficulties of the approach to its solution arise from the limitations of the developed noise-resistant treatments of hydroacoustic signals. Currently, interferometric processing, unlike other known processing methods, allows detecting and evaluating source parameters with greater noise immunity at low c/p ratios. This is due to two points.

Firstly, the processing implements multiple quasi-coherent accumulation of the spectral density of the wave field along localized interferogram bands in frequency-time variables. Secondly, at the output of the integral transformation, the spectral density of the signal is concentrated in a small region. The linear dimensions of this region are inversely proportional to the observation time, the width of the band and decrease with increasing radial velocity of the source. The smaller the

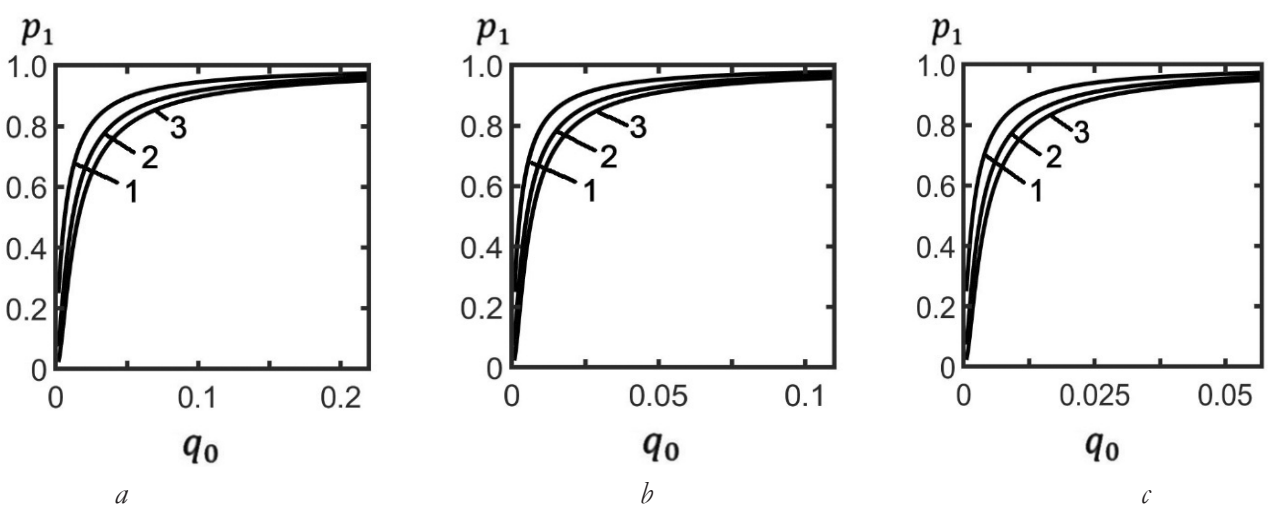

a *b* *c*

Fig. 4. *Dependence of the probability of correct detection p_1 on the input s/n ratio q_0 for different values of the false alarm probabilities p_2 and the number of antenna elements B. Curve 1 – p_2 = 0.1, curve 2 – p_2 = 0.01, curve 3 – p_2 = 0.001. B = 3 (a), B = 7 (b), B = 11 (c).*

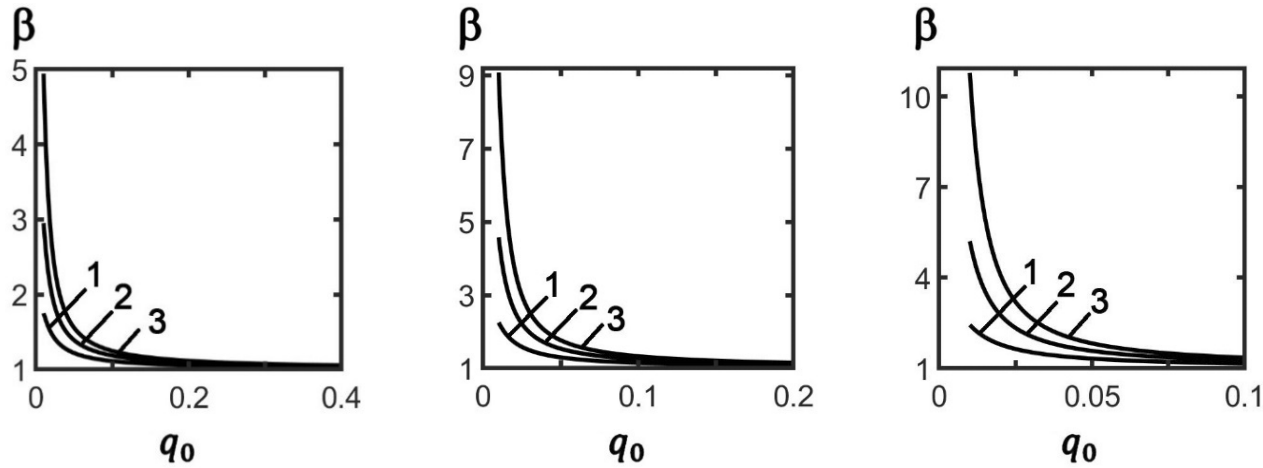

a *b* *c*

Fig. 5. *The dependence of the efficiency coefficient* β *on the input ratio s/n* q_0 *for different values of false alarm probabilities* p_2 *and the number of antenna elements B. Curve 1 –* $p_2 = 0.1$*, curve 2 –* $p_2 = 0.01$*, curve 3 –* $p_2 = 0.001$*. B = 3 (a), B = 7 (b), B = 11 (c).*

signal concentration area, the higher the noise immunity of the processing.

Based on interferometric processing, the detection of a noise source is considered by the Neumann-Pearson criterion by using a horizontal linear antenna. Analytical dependences of detection curves are obtained depending on the input s/n ratio and the number of antenna elements. Numerical calculations are performed. The efficiency of detecting a low-noise signal by an antenna in comparison with a single receiver is evaluated.

REFERENCES

1. Weston DE, Stevens KJ. Interference of wide band sound in shallow water. *J. Sound. Vib.,*1972, 21(1):57-64.
2. Chuprov SD. *The interference structure of the sound field in a layered ocean. In: Acoustics of Ocean. The current situation.* Moscow, Nauka Publ., 1982, pp. 71-82.
3. Kuperman WA, D'Spain GL. Ocean acoustic interference phenomena and signal processing. *AIP Conf. Proc. ed. by W.A. Kuperman and G.L. D'Spain.* 2002, N.Y., Melville.
4. Thode AM. Source ranging with minimal environmental information using a virtual receiver and waveguide invariant theory. *J. Acoust. Soc. Am.*, 2000, 108(4):1582-1594.
5. Quijanoa JE, Zurk LM, Rouseff D. Demonstration of the invariance principle for active sonar. *J. Acoust. Soc. Am.*, 2008, 123(3):1329-1337.
6. Tao H, Krolik JL. Waveguide invariant focusing for broadband beam forming in an oceanic waveguide. *J. Acoust. Soc. Am.*, 2008, 123(3):1338-1346.
7. Cocrell KL, Smidt H. Robust passive range estimation using the waveguide invariant. *J. Acoust. Soc. Am.,* 2010, 127(5):2780-2789.
8. Rouseff D, Zurk LM. Striation based beam forming for estimating the waveguide invariant with passive sonar. *J. Acoust. Soc. Am. Express Lett.*, 2011, 130(2):76-81.
9. Besedina TN, Kuznetsov GN, Kuz'kin VM, Pereselkov SA. Determining the depth of a sound source in a shallow sea against the background of intense noise. *Acoustical physics*, 2015, 61(6):718-728.
10. Kuznetsov GN, Kuzkin VM, Pereselkov SA. Spectrogram and localization of the sound source in the shallow sea. *Acoustical physics,* 2017, 63(4):406-418.
11. Kaznacheev IV, Kuznetsov GN, Kuzkin VM, Pereselkov SA. Interferometric method for detecting a moving sound source by a

vector-scalar receiver. *Acoustical physics,* 2018, 64(1):33-45.
12. Kuz'kin VM, Pereselkov SA, Kuznetsov GN, Kaznacheev IA. Interferometric direction finding by a vector-scalar receiver. *Phys. Wave Phenom.*, 2018, 26(1):63-73.
13. Kuz'kin VM, Kuznetsov GN, Pereselkov SA, Grigor'ev VA. Resolving power of the interferometric method of source localization. *Phys. Wave Phenom.,* 2018, 26(2):150-159.
14. Pereselkov SA, Kuz'kin VM, Kuznetsov GN, Prosovetsky DYu, Tkachenko SA. Interference method for estimating the coordinates of a moving noise source in a shallow sea using high-frequency signals. *Acoustical physics,* 2020, 66(4):437-445.
15. Kuz'kin VM, Lyakhov GA, Pereselkov SA, Matvienko YuV, Tkachenko SA. Noise-source detection in an oceanic waveguide using interferometric processing. *Phys. Wave Phenom.*, 2020, 28(1):68-74.
16. Caiti A, Munafo A, Vettori G. A geographical information system (gis)-based simulation tool to assess civilian harbor protection levels. *IEEE J. of Oceanic Engineering*, 2012, 37(1):85-102.
17. Kaznacheev IV, Kuz'kin VM, Kutsov MV, Lyakhov GA, Pereselkov SA. Interferometry in acoustic-data processing using extended antennas. Space–time analogy. *Phys. Wave Phenom.,* 2020, 28(4):326-332.
18. Brekhovskikh LM, Lysanov YuP. *Theoretical foundations of ocean acoustics.* Leningrad, Gidrometeoizdat Publ., 1982, 264 p.